ISSN 1392−1207. MECHANIKA. 2015 Volume 21(1): 5−10

A study on the effect of surface defect on the fatigue performance of metal component based on damage mechanics

Zhixin Zhan*, Weiping Hu, Miao Zhang***, Qingchun Meng*****
**BeiHang University, Beijing 100191, China, E-mail: zzxupc@163.com*
***BeiHang University, Beijing 100191, China, E-mail: huweiping@buaa.edu.cn*
****China Academy of Space Technology, Beijing 100094, China, E-mail: i42mg@163.com*
*****BeiHang University, Beijing 100191, China, E-mail: Qcmeng@buaa.edu.cn*

crossref http://dx.doi.org/10.5755/j01.mech.21.1.7923

1. Introduction

In the field of mechanical engineering, most engineering components are subject to cyclic load and fatigue failure [1] is one of the main failure modes, which is also an important factor related to the economy and security of structure in many engineering fields. The appearance of surface defect [2] makes this problem more complex as it has a significant influence on the fatigue behaviour of metallic materials. Many surface defects are generated due to accidental scratches and bumps in the process of product manufacturing and assembling and the forms of typical defects involve pits, scratches and other defects. It is important to study the effect of surface defect on the fatigue performance of metal components.

Many methods have been adopted to study the effect of surface defect on the fatigue behaviour. Benoit and Topper [3-4] present a method which defines a threshold of non-propagating crack around the defects empirically. The drawback of this method is that some parameters based on tests have to be empirically adjusted. The Kitagawa diagram [5] is another method, proposed by Kitagawa and Takahashi, which relates the evolution of fatigue limit with a function of defect size and it is established via amounts of results with respect to wide ranges of materials and defects. Murakami [6-7] proposes a model estimating the distribution of lifetime as a function of distribution of defect sizes, which is based on the crack initiation and propagation mechanics. The continuum damage mechanics approach is another method to analyse the fatigue behaviour of metal components, which has been proposed by Lemaitre and Chaboche [8-11]. The key point of the approach is constructing a damage evolution equation to reflect the fatigue damage evolution.

In this paper, a damage mechanics finite element method is used to study the effect of surface defect on the fatigue life of metal components. First, based on the continuum damage theory, the Lemaitre and Chaboche fatigue model is investigated in order to predict the fatigue life of metal components with defects. The parameters in the damage evolution equation are obtained with reference to the fatigue experimental data on the smooth and notched specimens. Then the finite element implementation of a continuum damage mechanics formulation for multiaxial fatigue is presented, in which the coupling relationship between the damage field and the stress field is taken into account. At last, the influence of surface defect on structure fatigue life is analysed from aspects of defect geometry and residual stress around the defect.

2. Fatigue damage model

2.1. Damage extent and constitutive relation

Based on continuum damage mechanics, some primary concepts have been proposed by Lemaitre and Chaboche [12]. For isotropic materials, the damage variable D is used to represent the stiffness deterioration under the fatigue load, which is reduced to a scalar variable: $D = D \cdot I$, where I is the second-order identity tensor, such as:

$$D = \frac{E - E_D}{E}, \tag{1}$$

where E is the Young's Modulus without damages and E_D is the Young's Modulus with damages. As E_D ranges from 0 to E, D varies between 0 and 1.

According to the elastic theory, the constitutive relation for isotropic materials with damage can be derived as:

$$\sigma_{ij} = (1-D)\delta_{ij}\lambda\delta_{kl}\varepsilon_{kl} + 2(1-D)\mu\varepsilon_{ij}, \tag{2}$$

where σ_{ij} and ε_{ij} stand for stress components and strain components, respectively. λ and μ are Lame Constants:

$$\lambda = \frac{E\nu}{(1+\nu)(1-2\nu)}, \mu = G = \frac{E}{2(1+\nu)}, \tag{3}$$

where ν is the Poisson ratio and G is the shear modulus.

In case of the uniaxial load, Eq. (2) is reduced to:

$$\sigma = E(1-D)\varepsilon. \tag{4}$$

2.2. Uniaxial fatigue damage model

In uniaxial cycle loading, based on remaining life and continuum damage concepts, the fatigue cumulative damage model can be illustrated as this form [13]:

$$\dot{D} = \frac{dD}{dN} = \left[1-(1-D)^{\beta+1}\right]^{\alpha(\sigma_{max},\sigma_m)} \left[\frac{\sigma_{max}-\sigma_m}{M(\sigma_m)(1-D)}\right]^{\beta}, \tag{5}$$

where D is the damage scalar variable and N is the number of cycles. σ_{max} and σ_m are, respectively, the maximum and mean applied stress. β is a material parameter. The expression of $\alpha(\sigma_{max},\sigma_m)$ is defined as:

$$\alpha(\sigma_{max},\sigma_m) = 1 - a\left\langle\frac{\sigma_{max}-\sigma_f(\sigma_m)}{\sigma_u-\sigma_{max}}\right\rangle, \tag{6}$$

$$\sigma_f(\sigma_m)=\sigma_{l0}+\sigma_m(1-b_1\sigma_{l0}), \quad (7)$$

where σ_u is the ultimate tensile stress, σ_{l0} is the fatigue limit for fully reversed conditions. a and b_1 are material parameters. The brackets $\langle\sigma\rangle$ are defined as $\langle\sigma\rangle=\sigma$ if $\sigma>0$ and $\langle\sigma\rangle=0$ if $\sigma\le 0$.

The expression of $M(\sigma_m)$ is defined as:

$$M(\sigma_m)=M_0(1-b_2\sigma_m), \quad (8)$$

where M_0 and b_2 are material parameters.

The number of cycles to failure N_F for an constant stress condition is obtained by integrating Eq. (5) from $D=0$ to $D=1$, leading to:

$$N_F=\frac{1}{1+\beta}\frac{1}{aM_0^{-\beta}}\frac{\langle\sigma_u-\sigma_{\max}\rangle}{\langle\sigma_{\max}-\sigma_f(\sigma_m)\rangle}\left(\frac{\sigma_a}{1-b_2\sigma_m}\right)^{-\beta}. \quad (9)$$

where σ_a is the stress amplitude during one loading cycle.

2.3. Multiaxial fatigue damage model

In the practical engineering application, the stress and strain are always multiaxial. The Lemaitre and Chaboche model has been extended to multiaxial loading by Chaudonneret [14]. The damage evolution law in the case of multiaxial loading is given as follows:

$$\dot{D}=\frac{dD}{dN}=\left[1-(1-D)^{\beta+1}\right]^{\alpha}\left[\frac{A_{II}}{M_0(1-3b_2\sigma_{H,m})(1-D)}\right]^{\beta}, \quad (10)$$

where A_{II} is the amplitude of octahedral shear stress, defined by:

$$A_{II}=\frac{1}{2}\left[\frac{3}{2}\left(S_{ij,\max}-S_{ij,\min}\right)\left(S_{ij,\max}-S_{ij,\min}\right)\right]^{1/2}, \quad (11)$$

where $S_{ij,\max}$ and $S_{ij,\min}$ are the maximum and the minimum values of the deviatoric stress tensor *ij* components during one loading cycle. $\sigma_{H,m}$ is the mean hydrostatic stress defined by:

$$\sigma_{H,m}=\frac{1}{6}\left[max(tr(\sigma))+min(tr(\sigma))\right], \quad (12)$$

with $tr(\sigma)=\sigma_{11}+\sigma_{22}+\sigma_{33}$. The parameter α is defined by:

$$\alpha=1-a\left\langle\frac{A_{II}-A_{II}^*}{\sigma_u-\sigma_{e,max}}\right\rangle, \quad (13)$$

where $\sigma_{e,max}$ is the maximum equivalent stress which is calculated by maximising the von Mise stress over a loading cycle. The Sines fatigue limit criterion A_{II}^* in this model is formulated by:

$$A_{II}^*=\sigma_{l0}(1-3b_1\sigma_{H,m}). \quad (14)$$

By integrating of Eq.(10) from $D=0$ to $D=1$ for an constant stress condition, the number of cycles to failure N_F is:

$$N_F=\frac{1}{1+\beta}\frac{1}{aM_0^{-\beta}}\frac{\langle\sigma_u-\sigma_{e,max}\rangle}{\langle A_{II}-A_{II}^*\rangle}\left(\frac{A_{II}}{1-b_2\sigma_{H,m}}\right)^{-\beta}. \quad (15)$$

3. Experiments and material parameters for LY7075

In order to obtain the damage evolution parameters for LY7075 aluminum alloy, fatigue experiments for smooth and notched specimens are conducted, and the geometries of which are shown in Figs.1 and 2 respectively. The diameter of bar is 7 mm for all smooth specimens and the elastic stress concentration factor K_T of the notched specimens is about 3.0. The chemical composition and the mechanics properties are presented in Tables 1 and 2. The fatigue tests of notched specimens were carried out at $R=-1$ and the fatigue tests of smooth specimens were carried out at three different values of stress ratio R(R = −1, 0.05 and 0.5).

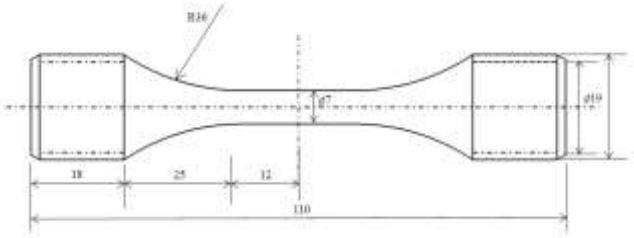

Fig. 1 Smooth specimen geometry (dimensions in mm)

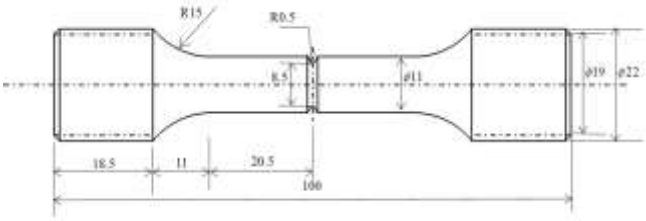

Fig. 2 Notched specimen geometry (dimensions in mm)

Table 1
Chemical composition of LY7075 (in weight percent)

Si	Fe	Cu	Mn	Mg	Cr	Zn	Al
0.40	0.50	1.20	0.30	2.90	0.18	5.50	89.02

Table 2
Static properties of LY7075

E, GPa	v	σ_b, MPa	σ_s, MPa
70	0.32	514	464

There are five parameters (β, α, M_0, b_1, b_2) in the damage evolution equation. The four material parameters (β, M_0, b_1, b_2) can be determined by the fatigue experimental data of smooth specimens. For the smooth specimens under the conditions of uniaxial fatigue loading, the S-N curve has been derived as shown in Eq. (9). When the fatigue tests are carried out at a fixed stress ratio, the relation between the number of cycles to failure N_F and the maximum stress σ_{max} can be obtained. Parameters β and $1/((1+\beta)aM_0^{-\beta})$ come from stress-controlled ($R=-1$) fatigue tests stress-life data. With the least square method, parameter b_1 and b_2 can be obtained from the fatigue tests

data at other different stress ratios ($R=0.05$, $R=0.5$).

In the present work, the independent parameters β and $aM_0^{-\beta}$ will be used in the incremental damage formulation and a is identified numerically, as the value which gives the same life for the incremental method. So one fatigue test data of notched specimens is needed to identify a . The fully reversed fatigue test data for the notched specimens, $R=-1$, $\sigma_{max}=100$ MPa ($\sigma_{\max}$ is the maximum nominal stress applied on the specimen) is used. Finally, the identified damage evolution parameters for LY7075 alloy are listed in Table 3.

Table 3
Material parameters of the Lemaitre and Chaboche fatigue damage model for LY7075

β	M_0	b_1	b_2	a
1.8462	74876.281	0.0014	0.0018	0.75

4. Computational methodology and simulations

4.1. Fatigue damage computation

The coupling relationship between the damage field and the stress field is taken into account by deploying APDL language on ANSYS platform [15-16] in finite element computation for the prediction of fatigue life.

The computational methodology is illustrated in the flowchart of Fig. 3, the subsequent damage is accumulated to predict the reduction in Young's modulus, using the following equation:

$$E^{(i+1)}=E(1-D^{(i+1)}). \tag{16}$$

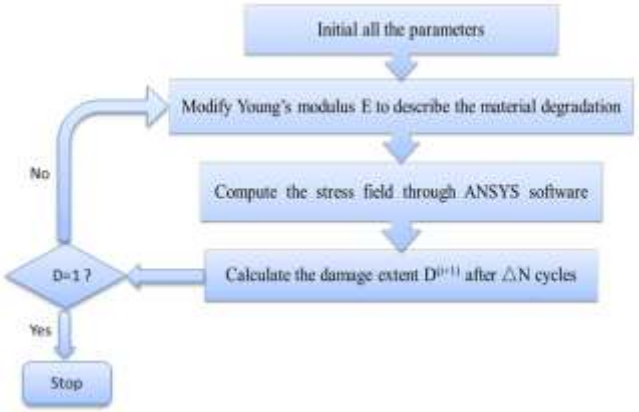

Fig. 3 The simplified FE computational methodology

The calculated amount is very expensive if we compute damage accumulation for every fatigue cycle. So ΔN is adopted to calculate the damage extent increment as follows:

$$\Delta D=\left[1-(1-D)^{\beta+1}\right]^{\alpha}\left[\frac{A_{II}}{M_0(1-3b_2\sigma_{H,m})(1-D)}\right]^{\beta}\Delta N\ , \tag{17}$$

then,

$$\Delta D^{(i+1)}=\Delta N\ D^{(i)}\ , \tag{18}$$

$$D^{(i+1)}=D^{(i)}+\Delta D^{(i+1)}. \tag{19}$$

When the accumulation of damage extent at any element reaches 1, fatigue crack initiation occurs at this element and the number of the cycles is the fatigue crack initiation life. This is the numerical solution for predicting the fatigue crack initiation lives.

4.2. Verification for the FE increment method

The specimen with defect is modeled for the validation of the approach. The geometric dimension of specimen with defect is shown in Fig. 4. The depth of the defect is 0.556 mm and the bottom corner radius is 0.168 mm. The defect morphology on the microscope is shown in Fig. 5.

Solid272 element is used to model axisymmetric specimens in the ANSYS platform. Each node of this kind of element has three degrees of freedom: translations in the nodal x, y, and z directions. The axisymmetric plane is created as shown in Fig. 6 and the actual FE mesh which is represented by the axisymmetric plane is shown in Fig.7. The cyclic loading is applied on the left side of the model and the boundary condition is applied on the right side as shown in Fig. 6. The maximum nominal axial stress applied on the defected specimen is 80MPa and the stress ratio R is 0.05. The distribution of axial stress on the notched specimen in the undamaged state is shown in Fig. 8. The change of damage extent versus number of cycles is shown in Fig. 9. The fatigue experiment results are listed in Table 4. The numerical solution obtained by FE increment method is 201000 and the experiment mean life is 194514. The outcome shows that the theoretical prediction tallies with the experimental results.

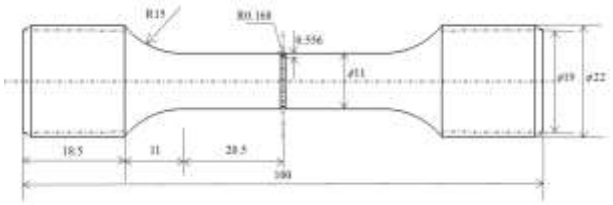

Fig.4 Specimens with defect geometry (dimensions in mm)

Fig. 5 Defect morphology on the microscope

Fig. 6 The axisymmetric plane of specimen

Fig. 7 The actual FE mesh of specimen with defect

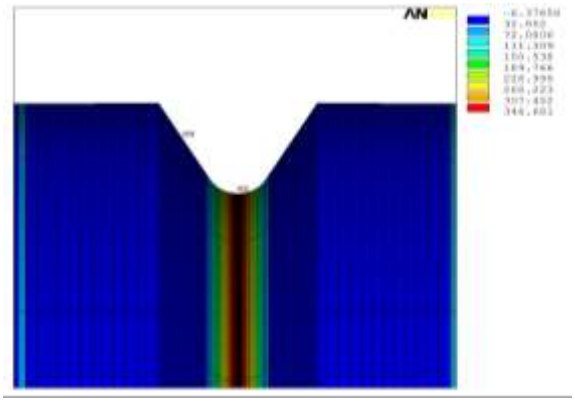

Fig. 8 Distribution of axial stress in the undamaged state

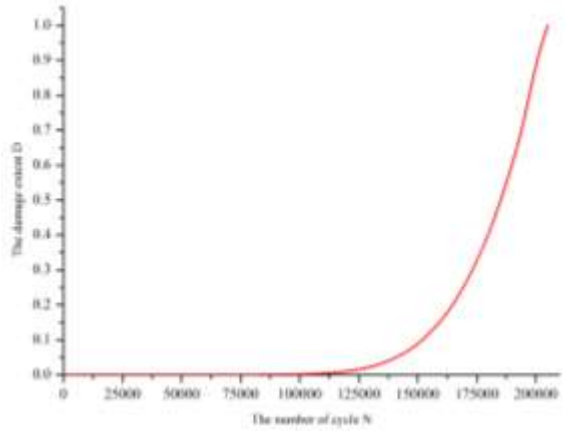

Fig. 9 The change of damage extent versus number of cycles

Table 4

Fatigue experiment results

Specimen No.	Fatigue life (cycle)
1	396884
2	79639
3	220201
4	88925
5	302114
6	92459
7	323642
8	366262
Mean life	194514

5. The influence of defect on the fatigue life

The influence of surface defects on the structural fatigue life mainly contains two aspects. One is the fatigue property of the material, and the other is the stress distribution in structures. The influence on the stress field also contains two aspects: one is the local stress concentration caused by the geometric shape of defect [17-18] and the other is the residual stress [19-20] field around the defect.

5.1. The influence of defect geometry size on the fatigue life

In order to analyse the influence of defect geometry size on the fatigue life, three kinds of size are designed and the shapes of defect are similar to that shown in Figs. 4 - 5. The depths of the defect are 0.556 mm, 0.321 mm and 0.051 mm, respectively, and the bottom corner radius is 0.168 mm. The FE numerical simulations are carried out at two different values of maximum nominal stress σ_{max} ($\sigma_{max} = 80.110$ MPa) with the same stress ratio R = -1. Figs. 10 and 11 show the axial and von Mises stress distributions for the three models with different depth of defects when the maximum nominal stress is 80MPa. The numerical solution obtained by FE increment method is shown in Table 5. The change of damage extent versus number of cycles when $\sigma_{max} = 80$ MPa is shown in Fig. 15.

From Fig.10 to Fig.12, we can see that the defect geometry size can make a significant influence on the stress distribution which is directly related to the damage evolution according to Eq. (10). The larger the defect is, the more severe the stress concentration around defect will be. Under the conditions of the same maximum nominal stress, the fatigue life decreases along with the increase of depth of defect.

Table 5

The numerical solution

Depth of defect, mm	σ_{max}, MPa	Fatigue life (cycle)
0.051	80	3885000
	110	1910000
0.321	80	555000
	110	89000
0.056	80	205000
	110	24000

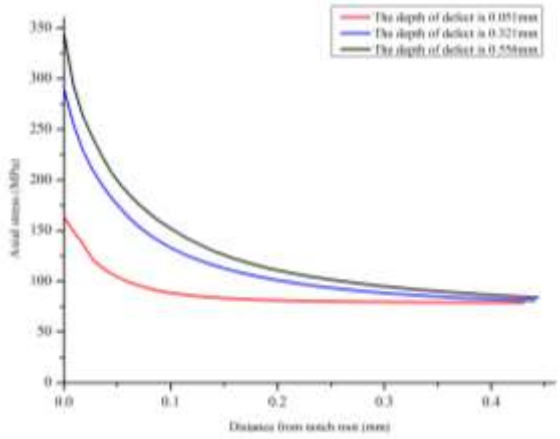

Fig. 10 Axial stress inward from the notch root when $\sigma_{n,max} = 80$ MPa

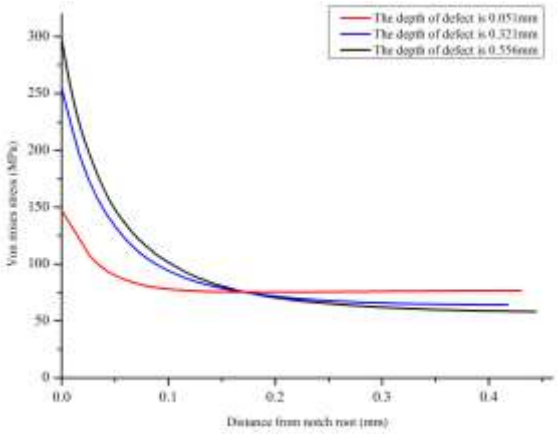

Fig. 11 Von Mises stress inward from the notch root when $\sigma_{n,max} = 80$ MPa

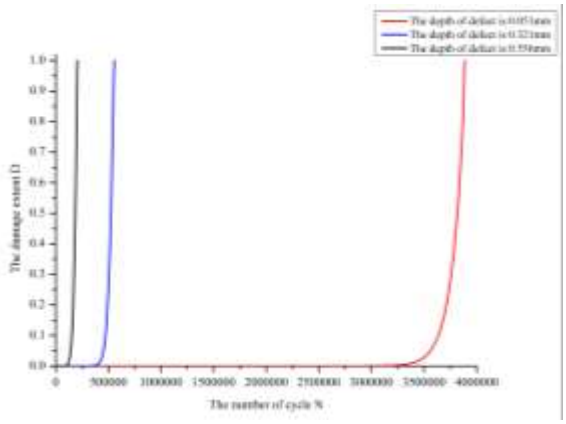

Fig. 12 The change of damage extent versus number of cycles when $\sigma_{n,max} = 80$ MPa

5.2. The influence of residual stress on the fatigue life

In practical application, the defect is often introduced unintentionally into components by impact or scrape. In this section, the finite element software LS_DYNA is used to simulate the generation of metal surface defects, which is similar to the simple metal cutting process.

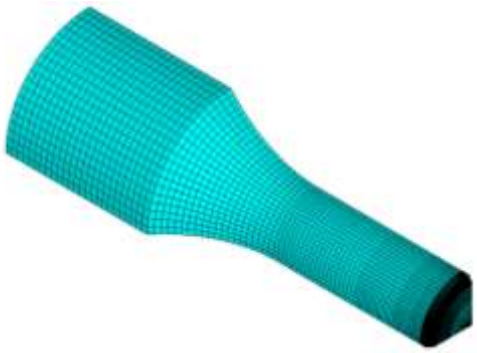

Fig. 13 The FE model after meshing

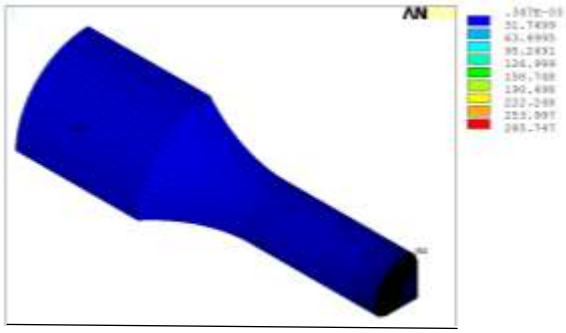

Fig. 14 Distribution of von Mises stress after cutting

The geometrical shape of the model after cutting is the same as shown in Fig. 4. In the ANSYS platform, only 1/8 of the specimen is built with the symmetry boundary conditions at the plane of symmetry. The FE model after meshing is shown in Fig. 13 and the equivalent stress obtained after cutting on the surface of the workpiece is shown in Fig. 14. We can see that the residual stress is mainly focused on the layer close to the surface of workpiece, which is caused by the poor thermal conductivity of aluminum alloy and the heat generated by the machining process mainly focus on the surface layer. The cycle maximum nominal stress is 80 MPa and the stress ratio R is 0.05. Finally, the numerical solution obtained by FE increment method is 105000. Fig. 15 shows two curves of relation between the change of damage extent and number of cycles, which are respectively corresponding to the model with residual stress and without residual stress.

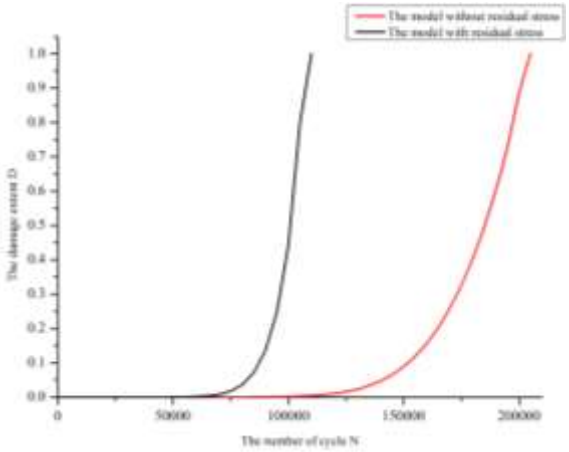

Fig. 15 The change of damage extent versus number of cycles

We can see that residual stresses can have a significant influence on the fatigue lives of components and the near surface tensile residual stresses can accelerate the initiation phase of the fatigue process. After the process of cutting, the residual stress is permanently present. When a cycle fatigue load is applied, the residual stress does not affect the stress amplitude, but it gives a shift to the mean stress. If the local residual stress is positive just as the example illustrated above, it increase the mean stress, which is unfavorable for fatigue according to Eq. (10) and the fatigue life is shorter than that without residual stress.

6. Conclusions

In this paper, based on the Chaboche nonlinear continuum damage model, the FE increment method is developed. According to the experiment results, this method is validated for multiaxial fatigue under the defected conditions. The method has been applied to analyze the influence of defect geometry size and residual stress on the fatigue life. Some of the main results can be summarized as follows:

- Based on the Chaboche nonlinear continuum damage model, the FE increment method is developed, which is applied to the life prediction of defected specimen.
- Based on the fatigue experimental results of standard smooth specimens and notched specimens, the damage evolution parameters are obtained.
- According to the damage evolution equation and damage evolution parameters, the fatigue life of the defected specimen is calculated, which is verified by the experiment results.
- The influence of defect geometry size and residual stress on the fatigue life has been analyzed. Under the conditions of the same maximum nominal stress, the fatigue life decreases along with the increase of depth of defect. The near surface tensile residual stresses can accelerate the initiation phase of the fatigue process.

References

1. **Schijve, J.; Schijve, J.; Schijve, J.** 2001. Fatigue of structures and materials: Springer.
2. **Bathias, C.; Pineau, A.** 2010. Fatigue of materials and structures: Wiley Online Library.
3. **Benoit, D.** 1981. Influence des Inclusions sur la Tenue en Fatigue des Aciers. Bibliographie review, 1RS1D Internai Report RFP; 301.
4. **El Haddad, M.; Topper, T.; Smith, K.** 1979. Prediction of non-propagating cracks, Engineering Fracture Mechanics 11(3): 573-84. http://dx.doi.org/10.1016/0013-7944(79)90081-X.
5. **Kitagawa, H.; Takahashi, S.** 1976. Applicability of fracture mechanics to very small cracks or the cracks in the early stage, Second International Conference on Mechanical Behavior of Materials ASM, Metals Park, Ohio: 627-631.
6. **Murakami, Y.** 2002. Metal fatigue: effects of small defects and nonmetallic inclusions: effects of small defects and nonmetallic inclusions: Elsevier.
7. **Murakami, Y.; Kodama, S.; Konuma, S.** 1989. Quantitative evaluation of effects of non-metallic inclusions on fatigue strength of high strength steels. I: Basic fatigue mechanism and evaluation of correlation between the fatigue fracture stress and the size and location of non-metallic inclusions, International Journal of Fatigue 11(5): 291-298. http://dx.doi.org/10.1016/0142-1123(89)90054-6.
8. **Chaboche, J-L.** 1981. Continuous damage mechanics–a tool to describe phenomena before crack initiation, Nuclear Engineering and Design 64(2): 233-247. http://dx.doi.org/10.1016/0029-5493(81)90007-8
9. **Kachanov, L.** 1986. Introduction to continuum damage mechanics: Springer. http://dx.doi.org/10.1007/978-94-017-1957-5
10. **Lemaitre, J.; Lippmann, H.** 1996. A course on damage mechanics: Springer Berlin.
11. **Yu SW.; Feng, X.** 1997. Damage mechanics. Tsinghua University Press: Beijing.
12. **Lemaitre, J.** 1994. Mechanics of solid materials: Cambridge university press.
13. **Chaboche, J.; Lesne, P.** 1988. A nonlinear continuous fatigue damage model, Fatigue & fracture of engineering materials & structures 11(1): 1-17. http://dx.doi.org/10.1111/j.1460-2695.1988.tb01216.x.
14. **Chaudonneret, M.** 1993. A simple and efficient multiaxial fatigue damage model for engineering applications of macro-crack initiation, Journal of engineering materials and technology 115(4): 373-379. http://dx.doi.org/10.1115/1.2904232.
15. **Zhang, M.; Meng, Q.C.; Hu, W.P.; Shi, S.D.; Hu, M.; Zhang X.** 2010. Damage mechanics method for fatigue life prediction of Pitch-Change-Link, International Journal of Fatigue 32(10): 1683-1688. http://dx.doi.org/10.1016/j.ijfatigue.2010.04.001.
16. **Zhang, T.; McHugh, P.; Leen, S.** 2012. Finite element implementation of multiaxial continuum damage mechanics for plain and fretting fatigue, International Journal of Fatigue 44: 260-272. http://dx.doi.org/10.1016/j.ijfatigue.2012.04.011.
17. **McEvily, A.; Endo, M.; Yamashita, K.; Ishihara, S.; Matsunaga, H.** 2008. Fatigue notch sensitivity and the notch size effect, International Journal of Fatigue 30(12): 2087-2093. http://dx.doi.org/10.1016/j.ijfatigue.2008.07.001.
18. **Sakane, M.; Zhang, S.; Kim, T.** 2011. Notch effect on multiaxial low cycle fatigue, International Journal of Fatigue 33(8): 959-968. http://dx.doi.org/10.1016/j.ijfatigue.2011.01.011.
19. **Webster, G.; Ezeilo, A.** 2001. Residual stress distributions and their influence on fatigue lifetimes, International Journal of Fatigue 23(1): 375-383. http://dx.doi.org/10.1016/S0142-1123(01)00133-5.
20. **Zhuang, W.Z.; Halford, G.R.** 2001. Investigation of residual stress relaxation under cyclic load, International Journal of Fatigue 23(1): 31-37. http://dx.doi.org/10.1016/S0142-1123(01)00132-3.

Zhixin Zhan, Weiping Hu, Miao Zhang, Qingchun Meng

A STUDY ON THE EFFECT OF SURFACE DEFECT ON THE FATIGUE PERFORMANCE OF METAL COMPONENT BASED ON DAMAGE MECHANICS

S u m m a r y

In order to study the effect of surface defect on the fatigue performance of metal component, the Lemaitre and Chaboche fatigue model is investigated. Then the finite element implementation of a continuum damage mechanics formulation for multiaxial fatigue is presented, in which the coupling relationship between the damage field and the stress field is taken into account. This FE method is validated according to the experimental results for defected multiaxial fatigue for LY7075. At last the influence of defect geometry size and residual stress on structure fatigue life is analysed.

Keywords: damage mechanics; residual stress; surface defect; multiaxial fatigue; fatigue life.

Received September 10, 2014
Accepted January 12, 2015